Ann. Inst. Statist. Math.
Vol. 46, No. 3, 405–428 (1994)

SEPARATION OF SPIN SYNCHRONIZED SIGNALS

T. HIGUCHI*, G. K. CRAWFORD, R. J. STRANGEWAY AND C. T. RUSSELL

Institute of Geophysics and Planetary Physics, University of California, Los Angeles, CA 90024-1567, U.S.A.

(Received March 16, 1992; revised November 17, 1993)

Abstract. In the measurements of VLF electric fields with the Pioneer Venus spacecraft in sunlight, spin synchronized signals often dominate over the naturally generated emissions. We present a method to separate natural emissions from the several possible sources of noise. Our major objective by this method is not to remove all spin modulation, but to effectively subtract the background noise caused by the identifiable noise sources. Examination of the data shows that the background spin synchronized noise is quite sensitive to $\theta(n)$, the angle between the sense axis and the solar direction. We model the observed data as $y(n) = w(n)t(n)f(\theta(n)) + x(n)$, where $f(\theta)$ represents the phase response of the background noise and $x(n)$ is the estimated natural emissions. $t(n)$ and $w(n)$ are the long-term trend component and time- and phase-independent component of the intensity of the background noise, respectively. The method to decompose $y(n)$ is based on the Bayesian approach which has been recently applied to various inversion problems such as nonstationary time series modeling and image reconstruction. In this procedure, the estimated parameters $w(n)$, $t(n)$, $f(\theta)$, and $x(n)$ can be determined automatically. We will describe the Bayesian scheme and its application to the Pioneer Venus VLF electric field data.

Key words and phrases: Time series, Bayesian approach, outlier detection, smoothing, nonlinear modeling.

1. Introduction

Data taken aboard a spinning spacecraft frequently suffers from an unwanted signals synchronized with the rotation of the spacecraft. If there is a strong noise source along some view direction, a resulting strong periodic noise appears in the measurements. We frequently face situations such that we cannot study the observed data without eliminating this periodic noise from the original data. It is therefore important to develop methods that can sufficiently separate the noise closely associated with spacecraft spin. Furthermore, an elimination of the noise is inevitably necessary in a case with an inversion involved in an analysis procedure,

* Now at the Institute of Statistical Mathematics, Tokyo 106, Japan.

because the periodic noise due to the spacecraft rotation is easily amplified by a simple inversion technique such as the direct differentiation of the observed data (Higuchi *et al.* (1988)). Hence we cannot avoid the problem of noise reduction when we examine data measured by a spacecraft.

Rocket observations to measure the altitude profile of the airglow are sometimes contaminated with a spurious modulation as well as noisy fluctuations (Higuchi *et al.* (1988), Kita *et al.* (1989)). Higuchi *et al.* (1988) had proposed a method to remove the spurious modulation as well as the noisy fluctuation by incorporating prior notions such that the spurious modulation could be locally approximated by a sinusoidal wave. Their scheme to incorporate prior information into the analysis process is based on the Bayesian approach to time series analysis by Akaike (1980). The scheme can be characterized both by explicitly modeling a time series in the time domain and by introducing an information criterion **ABIC** (Akaike Bayesian Information Criterion) which enables us to objectively define the tradeoff between prior information and goodness of fit of the model to data.

The Bayesian approach with ABIC has been extensively applied to a variety of statistical problems, after Akaike gave an explicit solution to the smoothing problem when both the prior and data distributions are Gaussian (Gersch and Kitagawa (1988)). Several prior models frequently used for normally disturbance-linear-stochastic regression are summarized in Higuchi (1991*a*). The broad applicability and simplicity of the Bayesian approach with ABIC naturally leads its application to a reduction of noise observed in satellite data (Higuchi (1991*b*)). Along the line proposed by Akaike, Kitagawa (1987) furthermore has generalized the basic Bayesian approach and extended its applicability to both non-Gaussian and non-linear time series models.

In the VLF electric field measurements from the Pioneer Venus spacecraft obtained in sunlight, spin-synchronized signals often dominate over naturally generated emissions. Consequently, the observed natural emissions are masked by sun-synchronous spacecraft noise sources. A method to separate natural emissions from the several possible sources of noise would greatly enhance the scientific return and help studies of very low frequency waves in the Venus ionopause and to test theories of various beam driven instabilities in front of the shock (Russell (1991), Strangeway (1991)). Our paper addresses this problem of separating the spin-synchronized signals in the Pioneer Venus wave data. A specific problem we are considering is the extraction of natural emission signal $x(n)$ from given data of the form

$$(y(n), \theta(n)) \qquad (n = 1, \ldots, N),$$

where the $y(n)$ are the observed electric fields and $\theta(n)$ is the angle between the sense axis of the antenna and the solar direction. This sense axis lies in the spin plane and joins the 2 cages of the antenna. In short, our purpose in this paper is to develop a method to automatically and objectively remove effects caused by the background noise which is closely associated with the spin phase θ. With this method we will be able to determine the role of plasma waves in the physics of the Venus ionosphere in situations in which we cannot now analyze the data because of the instrument noise levels.

The Pioneer Venus VLF instrument employs a short electric antenna with

a separation of the antenna cages of only 0.8 [m]. The antenna elements are capacitively coupled to the plasma (Scarf *et al.* (1980)). When the spacecraft is in sunlight the antenna rotates through an asymmetric photoelectron cloud and through the shadow of the spacecraft. Much of the analysis of VLF signal from this instruments has therefore been restricted to the portion of the orbit in which the spacecraft is in darkness such as the study of polarization of the VLF signals by Scarf and Russell (1988). The spin rate of the Pioneer Venus spacecraft is generally close to 13 [s] and the spin axis of the spacecraft is maintained perpendicular to the solar direction. Hence every 13 seconds the sensors rotate 360° around the spacecraft being in full sunlight most of the time but passing into partial, full and then partial eclipse again as the body mounted sensors are shadowed by the spacecraft. The electric field power in 4 narrow bands centered at 100 [Hz], 730 [Hz], 5.4 [kHz], and 30 [kHz] is measured at rates of up to 4 times per second, and logarithmically compressed before transmitting to Earth.

In Section 2 we propose a basic model for describing an observation $y(n)$. The concept and procedure to estimate the background noise are described in Section 3. In Section 4 we present a procedure to define a real signal $x(n)$. Some practical examples are shown in Section 5, and the final section discusses our results, pointing out some related work.

2. Observational model

Spin synchronized signals often dominate over the naturally generated emissions. As a result, the natural signals are masked by sun-synchronous spacecraft noise sources and the observed data are a superposition of the background noise and natural emissions. We therefore assume that the background noise $B(n)$ is linearly added to the real natural signal $x(n)$. Namely, we decompose the observed raw data $y(n)$ $(n = 1, 2, \ldots, N)$ into $B(n)$ (background noise) and $x(n)$ (real signal) as follows:

$$y(n) = B(n) + x(n). \tag{2.1}$$

Here it should be noticed that both $B(n)$ and $x(n)$ are positive valued, since they represent electric field spectral intensity measurements $((\mathrm{V/m})^2/\mathrm{Hz})$.

Examination of the data shows that the background noise is quite sensitive to the angle between the antenna sense axis and the solar direction, $\theta(n)$, so we assume that the background noise, $B(n)$, can be described as a function of time, n, and phase, $\theta(n)$: $B(n) = B(n, \theta(n))$. It should be remarked that the phase $\theta(n)$ is known previously. We show a typical example of the observed data $y(n)$, and phase $\theta(n)$, in Figs. 1(a) and (b), respectively. The data are the electric field spectral density for 5.4 [kHz] during four minutes on 7 Sep. 1986. The data are sampled at 0.25 second resolution ($\Delta t = 0.25$), and a time is shown in seconds starting from 20:00:00.370. The difference of phase of successive points in time, $|\theta(n) - \theta(n-1)|$, is either 6.90 or 6.91 [deg.] (round off error), and there is no simple function to describe a switch from one to another. As a result, a phase $\theta(n)$ is almost uniformly distributed, but irregularly spaced in phase domain from 0° to 360° [deg.]. Since the satellite spin provides the variation of phase $\theta(n)$ shown in

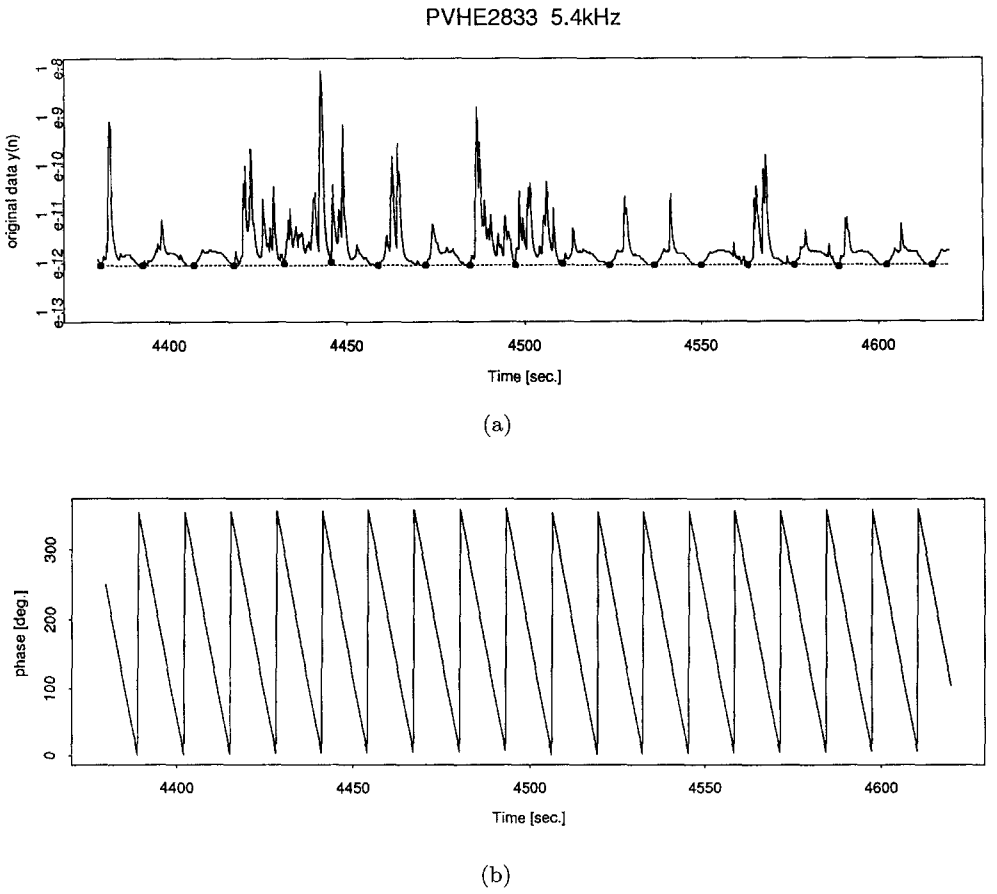

Fig. 1. (a) Raw observations of electric field spectral intensity measurements $((\mathrm{V/m})^2/\mathrm{Hz})$ for 5.4 [kHz]. The initial estimate for the long-term trend of the background noise intensity, $t^*_{(0)}$, is indicated by the broken line. (b) Phase variation (degree) as a function of time.

Fig. 1(b), the pattern associated with the background noise is highly repetitive in the time domain. The extremely large values seen in Fig. 1(a) are due to natural emissions ($B(n) \ll x(n)$).

A further complication is that the phase response of $B(n)$ is time-varying. However, this can be assumed to be gradually changing with time. Accordingly we model the observed data, $y(n)$, as

$$y(n) = I(n)f(\theta(n)) + x(n), \tag{2.2}$$

where $f(\theta)$ is the phase response (stationary part of the background noise) and $I(n)$ is the envelope of the background noise at each time n. Namely we assume that the background noise is modulated by the time-varying background noise intensity. This assumption is easily examined by plotting the observed data in the logarithmic scale, because equation (2.2) implies that data points without a natural

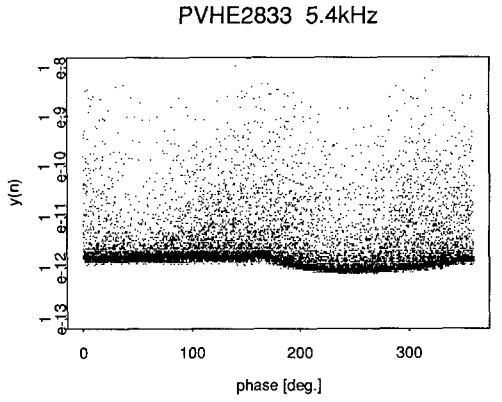

(a)

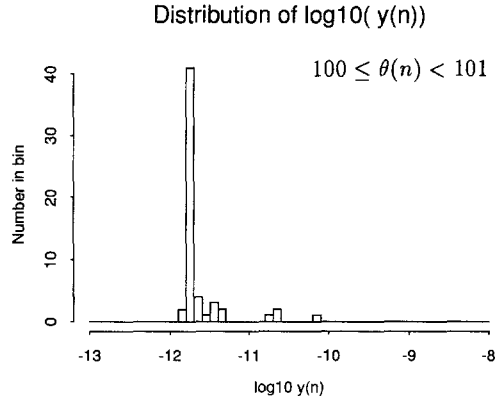

(b)

Fig. 2. (a) Observation $y(n)$ for 5.4 [kHz] in phase domain. (b) Histgram of $\log_{10} y(n)$ for $100 \leq \theta(n) < 101$.

emission ($x(n) = 0$) should scatter around $\log f(\theta)$ according to the logarithm of the time-varying background noise intensity, $\log I(n)$:

$$\log y(n) = \log I(n) + \log f(\theta(n)) \quad (\text{for } x(n) = 0). \tag{2.3}$$

We plot in Fig. 2(a) $\log y(n)$ during about 90 minutes ($N = 20394$) from 20:00:00.370 on the same day shown in Fig. 1, as a function of phase θ. The data points shown in Fig. 1(a) are also included in this figure. An envelope of minimum $\log y(n)$ at each θ roughly corresponds to the form of $\log f(\theta)$.

In order to confirm the above assumption, a histogram of $\log_{10} y(n)$ for $100 \leq \theta(n) < 101$ is shown in Fig. 2(b). It is clearly seen that the bulk of data points center at $\log_{10} y(n) = 12.2 \sim 12.3$. The small scatter around the peak of the histogram represents the fluctuation of $\log I(n)$, because the phase response $f(\theta)$ can be satisfactorily assumed to be constant within this phase range. In other words, the observation with the small difference of $\log y(n)$ from the peak of the histogram is assumed to be described as equation (2.3). In contrast, the data point isolated far from the bulk of the distribution of $\log_{10} y(n)$ is identified to contain

a real signal ($x(n) \neq 0$), because the fluctuation of the background noise intensity to provide such a large deviation from the peak is unlikely from a physical point of view.

3. Estimation of background noise

In this study, we will estimate the unknown form of $f(\theta)$ and $I(n)$. There is a significant problem which arises from the non-linearity of the background noise component $B(n, \theta) = I(n)f(\theta(n))$. Several possible treatments to mitigate this problem can be considered. The easiest approach is to separate a procedure into two steps: one is for estimating the form of $f(\theta)$ and the other is for $I(n)$. In this study, we basically adopt this procedure. First we roughly estimate the form of $f(\theta)$, removing the effect of $I(n)$ as much as possible. After this process, we estimate $I(n)$.

3.1 *Long term trend of the background noise intensity*

As mentioned above, we first estimate the form of $f(\theta)$, taking care of an effect from $I(n)$. If $I(n)$ is almost stationary and its mean is independent of time, we simply take an average of $\log y(n)$ for data points without the real signal in order to obtain the functional form of $\log f(\theta)$. However, our data shows that the mean of $I(n)$ sometimes drifts with time. We therefore eliminate this long-term trend of $I(n)$ before estimating $f(\theta)$. Here we further decompose $I(n)$ into two factors $I(n) = t(n)w(n)$, where $t(n)$ and $w(n)$ are a long-term trend and stationary component, respectively. By stationary component, we mean that the distribution can be assumed to be independent of time. Using this decomposition, equation (2.3) can be rewritten as follows:

$$\log y(n) = \log t(n) + \log w(n) + \log f(\theta) \quad (\text{for } x(n) = 0). \tag{3.1}$$

Moreover a variable of $\log y(n) - \log t(n)$ gives us an opportunity to estimate $\log f(\theta)$ without being disturbed by the nonstationarity of $I(n)$. Hence, we first calculate $t(n)$ before estimating $f(\theta)$.

The process of estimating $t(n)$ begins by determining the minimum background noise level for each individual spacecraft period. This provides a rough estimate of the variation in the background noise level, $\hat{t}(n)$, which is denoted by dots in Fig. 1(a). $\hat{t}(n)$ without a dot in this figure is treated as a missing value in our procedure. We assume that the long-term trend of the background noise intensity changes slowly with time. Hence an initial estimate for the long-term trend of the background noise intensity, $t^*_{(0)}(n)$, is defined by the smoothed $\hat{t}(n)$, where (0) explicitly indicates the estimation based on $\hat{t}(n)$. $t^*_{(0)}(n)$ is determined through the Bayesian smoothing technique with the simplest model which minimizes

$$\sum_n (\log \hat{t}(n) - \log t^*_{(0)}(n))^2 + \frac{1}{\tau_t^2}(\log t^*_{(0)}(n) - \log t^*_{(0)}(n-1))^2 \tag{3.2}$$

under given τ_t^2 (Higuchi (1991*b*)). The optimal value of the hyperparameter, τ_t^2, is, of course, determined according to the information criterion ABIC. We superpose

on Fig. 1(a) $t^*_{(0)}(n)$ by the broken line. The obtained $t^*_{(0)}(n)$ shows a straight line during this interval.

3.2 *Phase response function*

To estimate a phase response function of the background noise, we construct the following new time sequence

$$u(n) = \log y(n) - \log t^*_{(0)}(n) \tag{3.3}$$

which is little influenced by the long-term trend of the background noise intensity. If the observations contain no real signal, $u(n)$ can be rewritten as

$$\begin{aligned} u(n) &= \log w(n) + \log f(\theta(n)) \\ &= e(n) + \log f(\theta(n)), \qquad (\text{for } x(n) = 0) \end{aligned} \tag{3.4}$$

where we define $e(n) = \log w(n)$. As seen in Fig. 2(b), a distribution of $u(n)$ without real signal will scatter around $\log f(\theta)$ at each θ in the phase domain, according to the distribution of $e(n)$. As for the observations with significantly large real signal (as mentioned above, the real signal takes only positive values), the value of $u(n)$ is so far separated in value from $\log f(\theta)$ at each θ that it appears as an outlier in the phase domain. We estimate the form of $\log f(\theta)$ by using $u(n)$ derived from the observation $y(n)$ which is assumed to contain no real signal.

$\log f(\theta)$ takes various forms according to the location of the observations, and thereby the method to flexibly represent any functional form should be selected to express $\log f(\theta)$. Several methods to represent the form of $\log f(\theta)$ can be considered. In this study, we realize this problem to express $\log f(\theta)$ by the zero- or first-order spline (piecewise linear) representations. In this approach, $\log f(\theta)$ is specified by the number of segments, location of nodes, and the value at each node. Specifically, the following notation is used: the nodes are $\theta_i = i\Delta\theta$ $(i = 1, 2, \ldots, L(\Delta\theta))$, where $L(\Delta\theta)$ is the number of segments and given by $L(\Delta\theta) = 360/\Delta\theta$. The values at nodes are $\log f_i$. In our study, we set $\Delta\theta = 1$ and thus $L(\Delta\theta) = 360$. Furthermore, for simplicity, we adopt the zero-order spline function. So that a value of $\log f(\theta)$ within a range of $(i-1)\Delta\theta \leq \theta < i\Delta\theta$ (i-th bin) is represented by a single variable f_i.

As previously mentioned, we have to estimate $\log f_i$ by using only $y(n)$ without the real signal $x(n)$. Since it seems that most of the observations in our study can be attributed to only background noise, a limited number within individual bins which are so far separated in value from the remainder (bulk) behave as outliers. In order to cut out these outliers which probably contain real signal, we order the data within each bin according to increasing magnitude and denote the j-th largest within i-th bin by u_i^j; thus, $u_i^1 \leq u_i^2 \leq \cdots \leq u_i^{M_i-1} \leq u_i^{M_i}$ is the ordered set of observations within i-th bin, where the number of data points within i-th bin is specified by M_i. After rearranging the data in order of increasing magnitude, we find K_i values (out of a sample of size M_i) that are large when compared with the remaining $M_i - K_i$ values and define the rough estimate of $\log f_i$ by taking an average over the $M_i - K_i$ values of u_i^j.

This problem, a detection of an unknown number of multiple outliers, has received continued attention in the statistical literature. Much work has been done within the framework of traditional statistical hypothesis testing and the test proposed by Grubbs (1969) and the improved one based on his test are frequently used (Tietjen and Moore (1972)). Despite the simplicity of their method, there occurs three major flaws in their methods. First, we cannot identify even a single outlier in a case where several values are closer to each other than they are close to the bulk of the observations (Tietjen and Moore (1972)). This inability to detect an outlier is called "masking effect" of outliers. Second, we sometimes reject two large observations when only one outlier is actually present (Tietjen and Moore (1972), Kitagawa (1979)). Actually we have tried to apply Tietjen and Moore's method to our data and already confirmed its inability to detect the outliers, mainly due to the second reason. Finally, we do not know which significance level, e.g., 10%, 5%, or 1%, we should take in a framework of classical procedures (Kitagawa (1979)). Thus the procedures cannot be objective.

To overcome these difficulties, a Bayesian procedure has been proposed (Kitagawa and Akaike (1982)) and its practical utility has been illustrated by numerical examples. In their method, observations are assumed to obey a particular Gaussian distribution with ordered means such that $M_i - K_i$ observations $u_i^1, \ldots, u_i^{M_i-K_i}$ are the realization of normally distributed variables with an unknown common mean μ_i and variance σ_i^2, and K_i observations $u_i^{M_i-K_i+1}, \ldots, u_i^{M_i}$ are obtained from Gaussian distributions with ordered means, $\mu_i^{M_i-K_i+1} \leq \cdots \leq \mu_i^{M_i}$, and common variance σ_i^2. Namely, this model means that each outlier, which is assumed to contain a real signal, follows the Gaussian distribution with each mean, whereas the rest which are attributed to the background noise are normal observations drawn from the common Gaussian distribution. As for prior distribution, they assume that we have no information about the number of outliers. The readers are referred to Kitagawa and Akaike (1982) for the detailed derivations described above.

For a fixed value of K_i, the logarithm of the posterior probability that each outlier u_i^j is obtained from a distribution with each μ_i^j $(j = M_i - K_i + 1, \ldots, M_i)$, respectively, and that u_i^j $(j = 1, \ldots, M_i - K_i)$ is drawn from a distribution with common μ_i, is given by

$$\log p(K_i \mid u_i) = -\frac{M_i}{2} \log \sigma_i^2 - \frac{M_i(K_i+2)}{M_i - K_i - 3} - \log M_i! + \log(M_i - K_i)!, \tag{3.5}$$

where a common additive constant is ignored and

$$\sigma_i^2 = \frac{1}{M_i} \sum_{j=1}^{M_i-K_i} (u_i^j - \mu_i)^2, \qquad \mu_i = \frac{1}{M_i - K_i} \sum_{j=1}^{M_i-K_i} u_i^j. \tag{3.6}$$

The number of outliers, K_i, is in their method selected so as to maximize the posterior probability of u_i^j $(j = M_i - K_i + 1, \ldots, M_i)$ being the outliers. It should be noticed that this posterior probability is defined by summation of the posterior probability of $K_i!$ possible models, because there are $K_i!$ ways of assigning u_i^j

$(j = M_i - K_i + 1, \ldots, M_i)$ to the K_i distributions specified by the means μ_i^j $(j = M_i - K_i + 1, \ldots, M_i)$. For example, it is possible to consider the model such that $u_i^{M_i-1}$ and $u_i^{M_i}$ are generated from the distributions with the means of $\mu_i^{M_i}$ and $\mu_i^{M_i-1}$, respectively, whereas the rests of outlier u_i^j $(j = M_i-K_i+1, \ldots, M_i-2)$ are of course obtained from a distribution with μ_i^j $(j = M_i - K_i + 1, \ldots, M_i - 2)$, respectively. To calculate $K_i! - 1$ posterior probabilities except for equation (3.5) requires somewhat complicated numerical solution (Kitagawa and Akaike (1982)). Actually, unless there are outliers with nearly equal values, only the posterior probability of equation (3.5) takes a significant value among $K_i!$ models (Kitagawa and Akaike (1982)), and thus the posterior probability of u_i^j $(j = M_i - K_i + 1, \ldots, M_i)$ being the outliers is simply approximated by the posterior probability of equation (3.5), neglecting a contribution of the posterior probabilities of $K_i! - 1$ models. Since our data, as can be seen in Fig. 2(b), has also few outliers with the equal values within individual bins, we find the value of K_i to maximize equation (3.5), instead of calculating the definite posterior probabilities. After searching the optimal K_i, we define the rough estimate of $\log f_i$ by μ_i within individual bins; thus

$$\log \hat{f}_i = \frac{1}{M_i - K_i} \sum_{j=1}^{M_i-K_i} u_i^j. \tag{3.7}$$

Since $\log f(\theta)$ is assumed to show a smooth behavior in the phase domain, we define $\log f_i^*$ by smoothing the obtained $\log \hat{f}_i$. Here we also adopt a Bayesian smoothness approach which minimizes

$$\sum_{i=1}^{360} (\log \hat{f}_i - \log f_i^*)^2 + \frac{1}{\tau_f^2} (\log f_i^* - 2 \log f_{i-1}^* + \log f_{i-2}^*)^2 \tag{3.8}$$

under given τ_f^2, where f_0 and f_{-1} correspond to f_{360} and f_{359}, respectively. The used smoothing somewhat differs from that frequently used for a time series on the point that $f(\theta)$ is a periodic function, hence f_{360} should be connected to f_1 continuously. Naturally the value of τ_f^2 should be determined by ABIC. The obtained $\log f_i^*$ provides us with the phase response function $f_{(1)}^*(\theta)$, where the subscript (1) explicitly denotes the first estimate for the phase response function $f(\theta)$.

3.3 *Stationary component of variations of background noise intensity*

The defined $t_{(0)}^*(n)$ and $f_{(1)}^*(\theta)$ provide us with the initial estimate of the stationary component of the background noise intensity variation, $w_{(0.5)}^*(n)$, defined by

$$w_{(0.5)}^*(n) = \frac{y(n)}{t_{(0)}^*(n) f_{(1)}^*(\theta(n))}, \tag{3.9}$$

where a subscript (0.5) explicitly indicates the estimate by using $t_{(0)}^*(n)$ and $f_{(1)}^*(\theta)$. Of course, stationary components represent the stationary variation and its distribution is assumed to be characterized by a time-independent distribution function.

However, it sometimes occurs that there still remains in $w^*_{(0.5)}(n)$ an effect from the long-term trend of the background noise intensity variation, because $t^*_{(0)}(n)$ is the initial rough estimate for the long-term trend of the background noise intensity. Thus far, we adjust this initial estimate further by extracting the long-term trend from $w^*_{(0.5)}(n)$ if it exists.

Before subtracting the long-term trend in $w^*_{(0.5)}(n)$, we have to divide the total data set into two groups: candidates for $w^*_{(0.5)}(n)$ without the real signal and that which consists of the real signal and background noise. In short, we distinguish between the candidate for a pure background noise (designated hereafter by group-B) and that for a background noise + real signal (designated hereafter by group-$B+x$). While the sequences of $w^*_{(0.5)}(n)$ for the group-B almost show a stationary behavior in the time domain which can be characterized by a time-independent noise distribution function, $w^*_{(0.5)}(n)$ for the group-$B+x$ is much larger and behaves as an abrupt positive change in the sequences of $w^*_{(0.5)}(n)$. Therefore we extract the long-term trend in $w^*_{(0.5)}(n)$ by using only data from group-B.

The selection of the candidate data for group-B can be realized in this study by examining the distribution function of

$$e^*_{(0.5)}(n) = \log w^*_{(0.5)}(n), \tag{3.10}$$

because, as mentioned above, $e^*_{(0.5)}(n)$ for the group-$B + x$ appears as an outlier in a distribution function. The reason why we adopt $e^*_{(0.5)}(n)$ instead of $w^*_{(0.5)}(n)$ for selection is based on the fact that a distribution function of $e^*_{(0.5)}(n)$ for the group-B (hereafter we specify $p(e^*_{(0.5)})$) can be satisfactorily approximated by the normal (i.e., Gaussian) distribution which favors the smoothing by a linear Gaussian Bayesian approach. When $e^*_{(0.5)}(n)$ is less than the threshold $e_{\max}$, $y(n)$ is classified as a candidate for the group-B. On the contrary, $y(n)$ with $e^*_{(0.5)}(n)$ larger than $e_{\max}$ is considered to be an outlier and classified as the candidate for the group-$B + x$.

To divide the data into two groups, it still remains a problem to choose $e_{\max}$. As previously mentioned, the real value (i.e., natural emission) takes only positive value, and thus $y(n)$ with the smallest $e^*_{(0.5)}(n)$, $e_{\min}$, can be definitely attributed to the group-B. Of course, if the data with the smallest value of $e^*_{(0.5)}(n)$ is obviously attributed to the local and occasional artificial noise, we define $e_{\min}$ among the rest by excluding it. Furthermore, many examinations of data show that $p(e^*_{(0.5)})$ appears to be symmetric with respect to its peak. Hence, we define the threshold $e_{\max}$ by $e_{\max} = e_{\min} + 2(e_{\text{peak}} - e_{\min})$, where e_{peak} is determined by $e^*_{(0.5)}$ at which $p(e^*_{(0.5)})$ shows a sharp peak. The value of e_{peak} is easily determined by searching the peak of histogram of $e^*_{(0.5)}(n)$, because the number of $e^*_{(0.5)}(n)$ is large enough in our study to approximate its distribution by the histogram.

An extraction of the long-term trend component can be realized by simply smoothing $e^*_{(0.5)}(n)$ of the candidate for the group-B. The slowly changing variation obtained by this smoothing is also considered to be the long-term trend component. In the smoothing procedure, $e^*_{(0.5)}(n)$ for the group-$B + x$ is treated as missing value. Of course, the linear Bayesian approach is adopted for smoothing once again and the long-term trend is objectively and automatically estimated

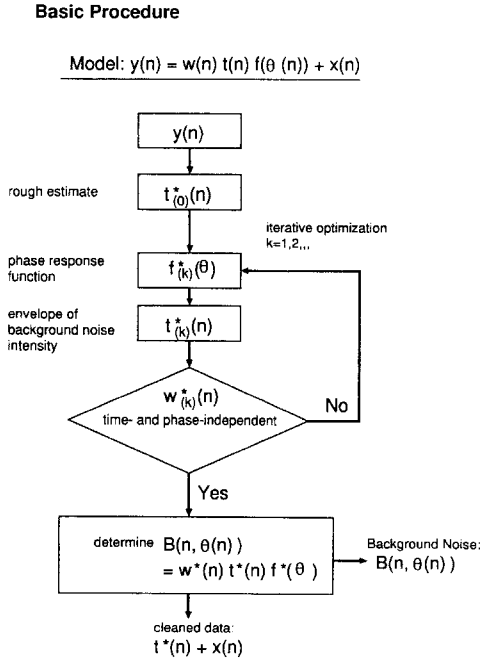

Fig. 3. Illustrating the flow of the algorithm.

according to ABIC. In this case, we adopt the simplest model as in equation (3.2) (Higuchi (1991*a*)). The smoothed $e^*_{(0.5)}(n)$, hereafter denoted by $\tilde{e}^*_{(0.5)}(n)$, is attributed to the long-term trend. Hence we correct the initial estimate for the long-term trend, $t^*_{(0)}(n)$, by

$$\begin{aligned} \log t^*_{(1)}(n) &= \log t^*_{(0)}(n) + \tilde{e}^*_{(0.5)}(n) \\ &= \log t^*_{(0)}(n) + \log \tilde{w}^*_{(0.5)}(n), \end{aligned} \tag{3.11}$$

where $\tilde{w}^*_{(0.5)}$ is given by $\exp(\tilde{e}^*_{(0.5)})$. Accordingly, the corrected stationary component of the background noise intensity variation is given by

$$\begin{aligned} \log w^*_{(1)}(n) &= e^*_{(0.5)}(n) - \tilde{e}^*_{(0.5)}(n) \\ &= \log w^*_{(0.5)}(n) - \log \tilde{w}^*_{(0.5)}(n). \end{aligned} \tag{3.12}$$

It should be noticed that no estimate of $\log w^*_{(1)}(n)$ is given as for the candidate for the group-$B + x$, because the value of $e^*_{(0.5)}(n) = \log w^*_{(0.5)}(n)$ is treated as missing in smoothing process. Even when $\log w^*_{(0.5)}(n)$ is from the group-$B+x$, the corrected long-term trend $t^*_{(1)}(n)$ can be defined due to an automatic interpolation of the missing value; i.e., $\tilde{e}^*_{(0.5)}(n)$ is defined at all n.

3.4 *Iterative optimization*

By using the corrected long-term trend component, $t^*_{(1)}(n)$, we can further adjust the phase response function form by returning to the procedure explained

in Subsection 3.2. In short, we replace $t^*_{(0)}(n)$ in equation (3.3) with $t^*_{(1)}(n)$ and successively continue the following procedures shown in Subsections 3.2 and 3.3. Consequently, we can get the second estimate for the phase response function $f^*_{(2)}(\theta)$ and the third estimate for the long-term trend component $t^*_{(2)}(n)$. We repeat these iterative improvements for $t^*_{(k)}(n)$ and $f^*_{(k)}(\theta)$ until the distribution function of $\log w^*_{(k)}(n)$ can be satisfactorily assumed to obey the time-independent noise distribution, where k designates the number of iteration. Practically, this iteration is stopped at proper k. We specify the estimate of $t^*_{(k)}(n)$ and $f^*_{(k)}(\theta)$ at this chosen k by $t^*(n)$ and $f^*(\theta)$, respectively. In the actual application to our data, we need only a few iterations and can get the satisfactory estimation for $t^*(n)$ and $f^*(\theta)$ at one or two iterations. The proposed approach is illustrated diagrammatically in Fig. 3.

4. Estimation of real signal

Based on the final estimates of $t^*(n)$ and $f^*(\theta)$, the estimation of the real signal begins by dividing the observations into two groups: candidates for the pure background noise (group-B) and that for the background noise + real signal (group-$B+x$). As in Subsection 3.3, this classification is also realized by examining the logarithm of the stationary component in the background noise intensity variation, $\log w^*(n)$, which is defined by

$$
\begin{aligned}
(4.1) \qquad e^*(n) &= \log w^*(n) \\
&= \log y(n) - \log t^*(n) - \log f^*(\theta(n)).
\end{aligned}
$$

The observations in our data are highly contaminated with the background noise and most of them are assumed to be classified into the group-B. Furthermore, the distribution of $e^*(n)$ for this candidate has a narrow central peak and seemed to be well approximated by the normal distribution. As for the candidate for the group-$B+x$, $e^*(n)$ is much larger than the mean of the group-B. Namely, $e^*(n)$ of the group-$B+x$ is always far from the bulk of the group-B, and appears to behave as an outlier. Hence, we classify the observations according to the following criteria. If $e^*(n)$ is larger than $e^*_{\max}$, $y(n)$ is assumed to be the candidate which contains a real signal (group-$B+x$). $y(n)$ with $e^*(n)$ less than $e^*_{\max}$ is classified into the candidate for the pure background noise (group-B).

There also remains a problem to choose $e^*_{\max}$. As previously mentioned, $e^*(n)$ of the group-$B+x$ is much larger, at least about a few times the standard deviation (σ_B) which is defined by the standard deviation of the group-B. In our study, the optimal choice for $e^*_{\max}$ does not require a procedure for the statistical test. We simply set $e^*_{\max}$ by simply examining the histogram of $e^*(n)$ and define its value by $e^*_{\max} = e^*_{\min} + 2(e^*_{\text{peak}} - e^*_{\min})$ as in Subsection 3.3, where e^*_{peak} and $e^*_{\min}$ are the peak and minimum value of the distribution of $e^*(n)$, respectively.

According to above criteria, the real signal $x(n)$ is estimated by

$$
(4.2) \qquad x(n) = y(n) - t^*(n) f^*(\theta(n)),
$$

for $e^*(n)$ larger than $e^*_{\max}$. This definition of the real signal is based on the assumption that $w^*(n) = 1$ for $e^*(n)$ larger than $e^*_{\max}$. Here we define the *cleaned data* by

$$y^*(n) = t^*(n) + x(n), \tag{4.3}$$

which is free both from the phase effect and from the stationary fluctuation of the background noise intensity. Obviously, for $e^*(n)$ less than $e^*_{\max}$, $x(n)$ should be zero. This cleaned data basically represents the long-term trend of the background noise intensity, and sometimes shows an additional real signal if one is observed.

5. Examples

The electric field spectral intensity $y(n)$ is simultaneously measured in four bands: 100 [Hz], 730 [Hz], 5.4 [kHz], and 30 [kHz]. The background noise level of observation for the highest band (30 [kHz]) is too low to require a statistical approach presented above. We therefore focus on the lowest three bands in this study and apply our approach to them. Before showing results of our procedure, we remark that the ratio of the signal to background noise evidently becomes lower with decreasing frequency of the measured electric field intensity. Our demonstration begins by showing the result applied to the easiest problem among three bands, 5.4 [kHz].

5.1 5.4 [kHz]

In Section 2, we explained the basic model for observation by using the data set measured for 5.4 [kHz]. The initial estimate of the long-term trend component, $t^*_{(0)}(n)$, for this data set has been already shown in Fig. 1(a). Accordingly it is worth while presenting the initial estimate of the phase response function, $f^*_{(1)}(\theta)$, for this data set in order to illustrate an outline of our approach. We show the rough estimate for the phase response function, $\hat{f}_i$, and its smoothed one, f^*_i, in Figs. 4(a) and (b), respectively. It should be noticed that the minimum value of $\hat{f}_i$ ($\hat{f}_i \sim 1$) is caused by a subtraction of $\log t^*_{(0)}(n)$ from $\log y(n)$; i.e., $\hat{f}_i$ is dimensionless variable. Comparing the top panel with Fig. 2(a) indicates that our simple approach to roughly estimate the phase response function for the background noise works very well. In short, we can satisfactorily eliminate an effect of the data point with real signal in a process of estimating the phase response of the background noise. Seemingly there is no difference between panels (a) and (b). However, f^*_i shows smoother behavior than $\hat{f}_i$. In this case, the value of hyperparameter, τ^2_f, is set 1, according to ABIC.

The obtained $t^*_{(0)}(n)$ and $f^*_{(1)}(\theta)$ generate the time series of an initial estimate of the stationary component of the background noise intensity variation, $w^*_{(0.5)}(n)$. If there still remains a long-term trend in $w^*_{(0.5)}(n)$, we furthermore remove it from $w^*_{(0.5)}(n)$ and correct the initial estimate of the long-term component, according to the procedure explained in Subsection 3.3. Actually we can get a satisfactory result for the estimation of the background noise at this stage. As previously mentioned, we can pursue an iterative procedure by calculating $f^*_{(2)}(\theta)$ based on

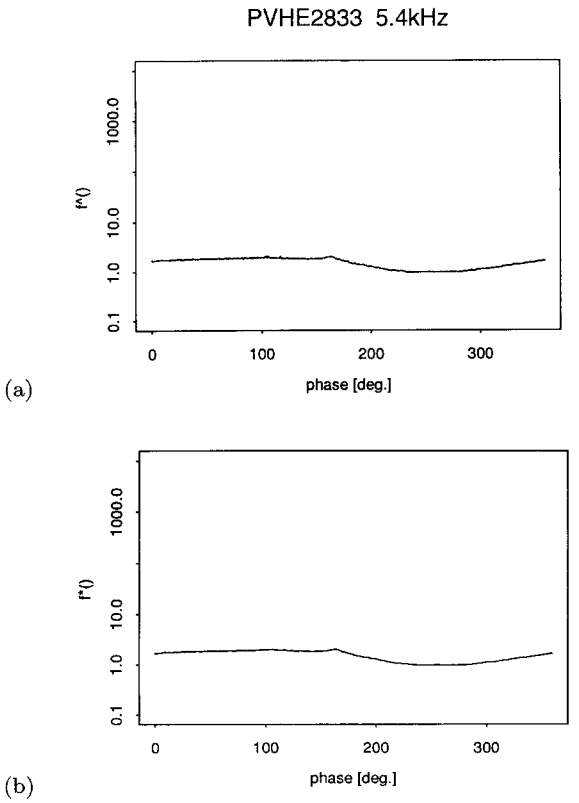

Fig. 4. (a) Rough estimate for the phase response function, $\hat{f}_i$, for the data set shown in Fig. 2(a). (b) The smoothed phase response function, f_i^*.

$t^*_{(1)}(n)$. This iteration should be continued until the derived stationary component can be assumed to obey the time–independent noise distribution function.

We show in Fig. 5(a) the cleaned data, $t^*(n) + x(n)$, in which neither an effect of the phase response of the background noise nor that from a stationary component is included. The final estimate for the long-term trend component, $t^*(n)$, is also demonstrated in the bottom panel, Fig. 5(b). The final estimates for all variables are obtained at one iteration: for example, $t^*(n) = t^*_{(1)}(n)$. The demonstrated interval for both panels is the same as that in Fig. 1. We can see in Fig. 5(a) that the cyclic pattern identified in the original time series $y(n)$, which is closely associated with the phase change, is clearly removed in the cleaned data. A slight difference of $t^*(n)$ from $t^*_{(0)}(n)$ stems from quite minor correction for the long-term component estimation.

Plotting the cleaned data $t^*(n) + x(n)$ in the phase domain greatly enhances the understanding of our procedure to eliminate an effect of the background noise on phase in the phase domain. Figure 6 shows the cleaned data for data points shown in Fig. 2(a). We can no longer see in this figure the dependence of the background noise on phase, which appears in the phase domain as the change in minimum level of $y(n)$ as a function of phase. By our formulation to extract

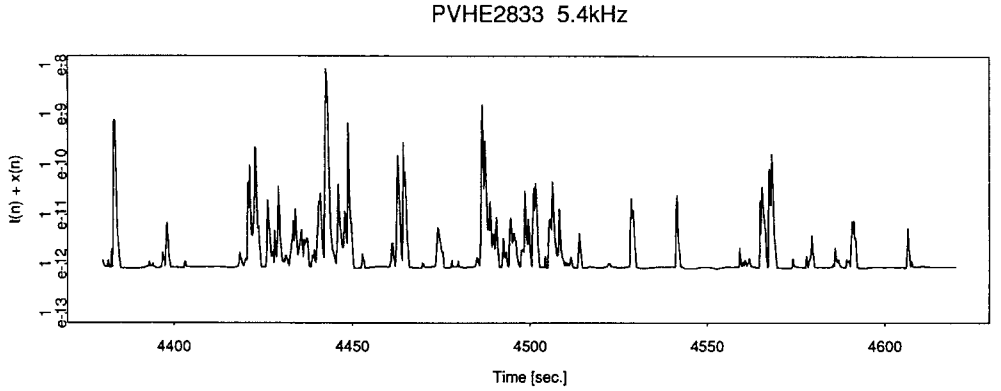

(a)

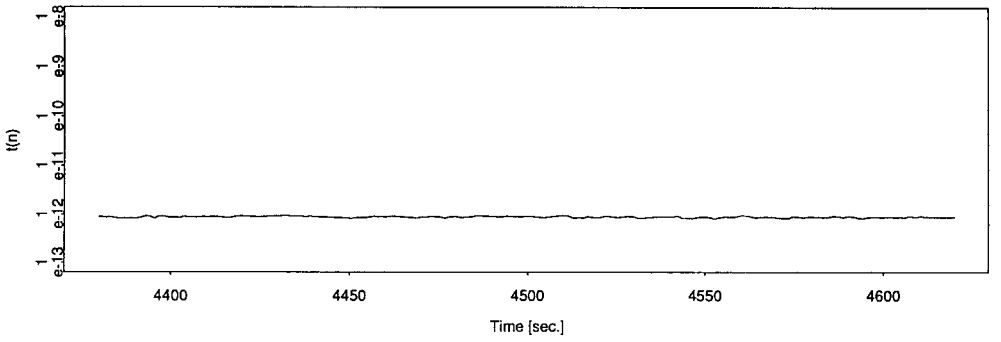

(b)

Fig. 5. (a) The cleaned data, $t^*(n) + x(n)$, for the data set shown in Fig. 1 in time domain. (b) The final estimate for the long-term component of the background noise intensity variation, $t^*(n)$.

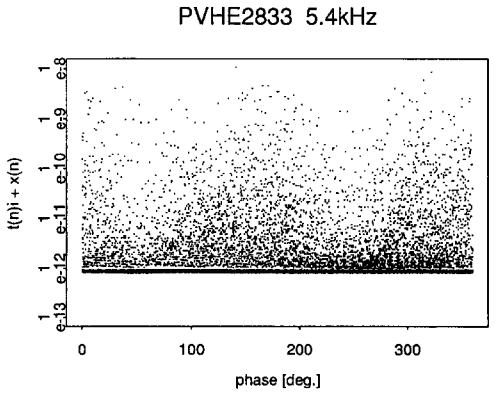

Fig. 6. The cleaned data, $t^*(n) + x(n)$, for the data set shown in Fig. 2(a) in phase domain.

the effect of $f^*(\theta)$ from $y(n)$, the cleaned data without real signal (i.e., $t^*(n)$) is defined so as to represent a minimum background noise intensity level. The estimated $t^*(n)$ shows an almost constant pattern during an interval (about one hour) in which this data set PVHE 2833 was obtained, but slowly changes as time goes. This change in $t^*(n)$ leads a very small fluctuation of the cleaned data with $x(n) = 0$ in phase domain, around an average of $t^*(n)$ with $x(n) = 0$, as seen in figure. Naturally the variance of this fluctuation is smaller than that of $y(n)$ without real signal which is seen in Fig. 2(a), because the cleaned data contain no stationary component of the variation of the background noise intensity.

5.2 730 [Hz]

To extract the phase dependence of the background noise for 730 [Hz] becomes more difficult than that for 5.4 [kHz], because of its reduced signal to noise ratio compared with that for 5.4 [kHz]. In addition, the more complicated form of the background noise as a function of phase makes it more difficult to remove an effect of the background noise associated with phase. We demonstrate in Fig. 7(a) the observation $y(n)$ for 730 [Hz] in the phase domain. This data set was measured during the same interval as that for 5.4 [kHz] shown in Fig. 2(a). An envelope of the minimum observation as a function of phase corresponds to the dependency of the background noise on phase. We demonstrate in Fig. 7(b) the estimated phase response function $f^*(\theta)$ which is obtained at an iteration number $k = 1$: $f^*(\theta) = f^*_{(1)}(\theta)$. The good performance of our procedure to estimate $f^*(\theta)$ even for 730 [Hz] can be easily understood by superposing panel (b) onto panel (a).

Before showing the cleaned data, we notice in panel (a) a rapid rise of $y(n)$ within the limited phase range between 160 and 190 [deg.], in particular between 178 and 190 [deg.]. Because of slight valiability in the onset of the rapid rise, it cannot be adequately represented as the background noise by equation (2.3). We have examined in detail both the time- and phase-dependence of this scatter within this phase range, but no dependency was found. Thus, the following special treatment is required: no data within this phase range is used to determine the stationary component of the background noise as discussed in Subsection 3.3, even though it is classified as the group-B. In addition, the cleaned data within this phase range is *a priori* defined to contain no real signal and is excluded from our analysis. We demonstrate the cleaned data in Fig. 7(c). As mentioned above, only data points without $x(n)$ can be seen within the range from 160 to 190 [deg.]. It should be emphasized that the special treatment like this is seldom applied and that our model expressed by equation (2.3) is basically appropriate for representing the background noise.

We show a part of this cleaned data in time domain. Figures 8(a) and (b) are the original observation and the cleaned data, respectively. In this case, it is nearly impossible to extract useful information without removing the background noise from $y(n)$. Panel (b) suggests that the cleaned data provide us an opportunity to examine the data set strongly contaminated with spin synchronized noise. It is interesting that the final estimate for the long-term component $t^*(n)$ is almost constant during this interval.

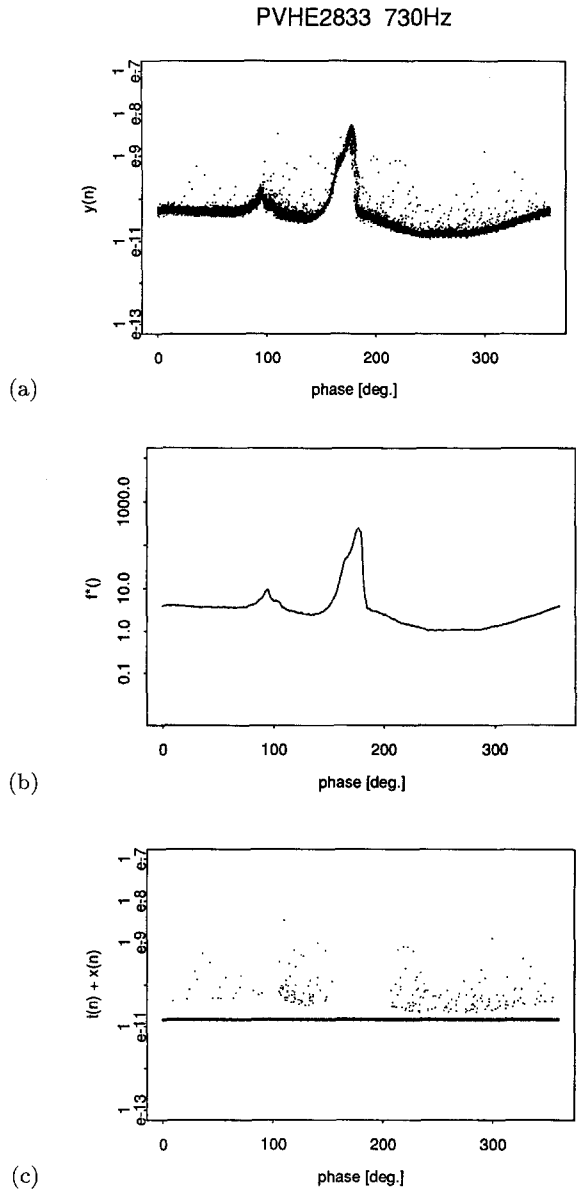

Fig. 7. (a) Observation $y(n)$ for 730 [Hz] in phase domain. (b) The smoothed phase response function, f_i^*. (c) The cleaned data, $t^*(n) + x(n)$.

5.3 100 [Hz]

Finally we show a result of our procedure applied to the most difficult problem, 100 [Hz]. The applied data set was obtained during about 24 minutes from 20:00:00:370 to 20:23:20:382 on 14 May, 1979 and the number of data points is $N = 5600$. The sampling time Δt is also 0.25 second. We plot the original observations from 20:00:00:370 to 20:21:39:391 in the phase domain in Fig. 9(a). The

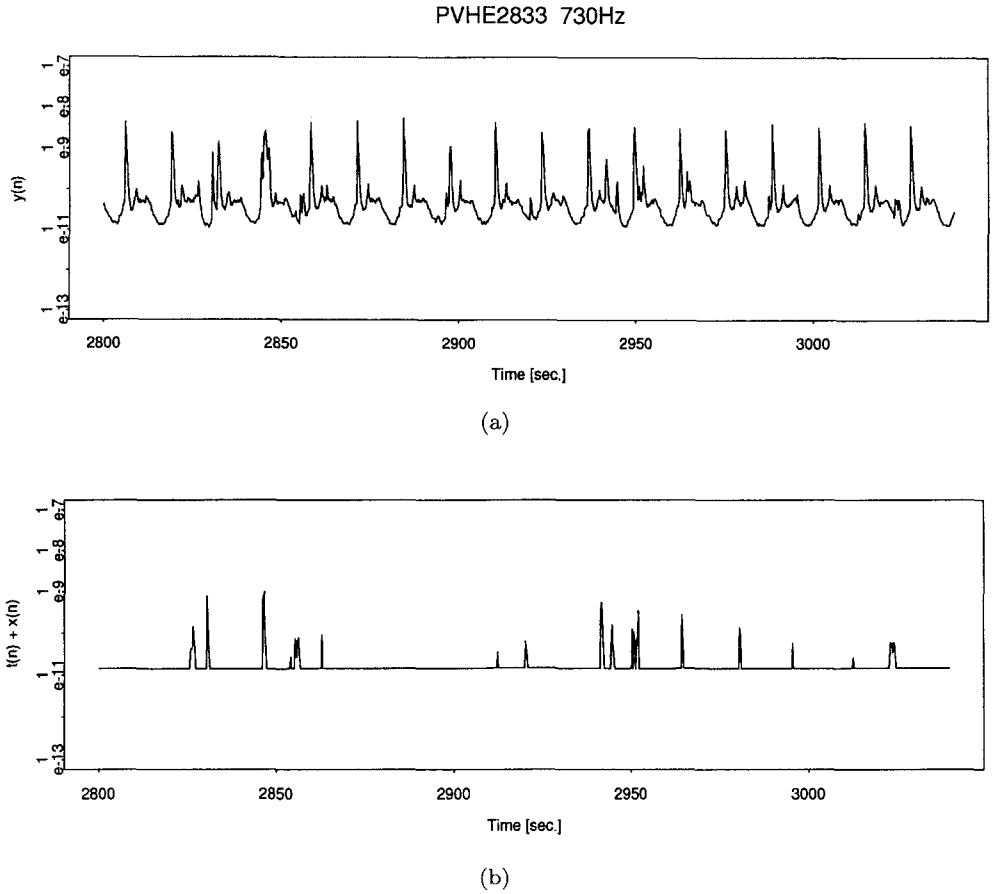

Fig. 8. (a) Observation $y(n)$ for 730 [Hz] in time domain. (b) The cleaned data, $t^*(n)+x(n)$.

data points obtained after 20:21:39.391 are not shown in this figure, because an effort to visually grasp the characteristics of the background noise in phase domain is hampered by a large increase in the background noise level after this time, which is shown in Fig. 10(a). We plot the observations in the time domain in Fig. 10(a) from 20:19:20:379 through 20:23:20:382. The time is indicated in seconds starting from time of 20:00:00:370. An enhancement of the background noise level is clearly seen in this figure after about $t = 1370$ [sec.]. We therefore plot no data point after this time in Fig. 9(a) in order to easily capture the basic feature of the background noise in phase domain.

It is seen in Fig. 9(a) that the ratio of signal to background noise is still lower compared with that for 730 [Hz]. This small ratio makes it difficult to distinguish the data points with a real signal from those composed only of the background noise. The estimated phase response function is shown in Fig. 9(b). The relatively rough behavior of this curve is produced by larger variation of the background noise intensity both in time and in phase domains. We show in Fig. 9(c) the cleaned

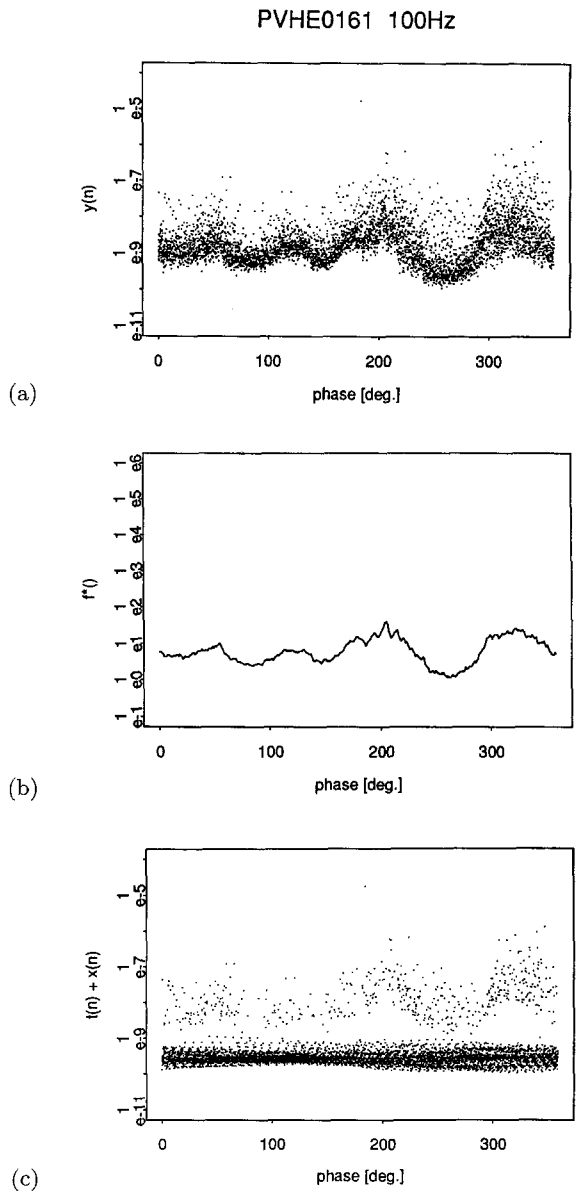

Fig. 9. (a) Observation $y(n)$ for 100 [Hz] in phase domain. (b) The smoothed phase response function, f_i^*. (c) The cleaned data, $t^*(n) + x(n)$.

data in the phase domain. Similarly no point after 20:21:39.391 is demonstrated in panel (c). Even for this case, we can extract data points seeming to contain a real signal, with removing an effect from the background noise. It should be remarked here that the outline of the blank area seen in this panel, which lies between the bulk of group-B points and of group-$B + x$, is obviously related to the signature of $f^*(\theta)$. This dependency stems from the definition for classification of data into

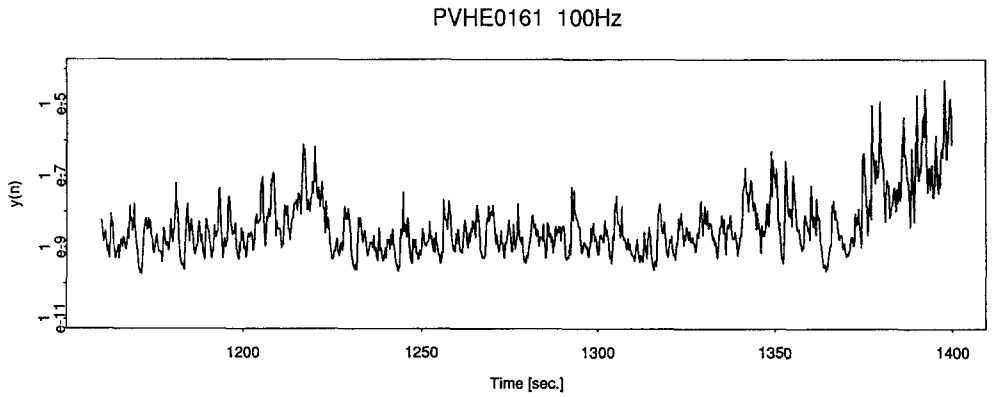

(a)

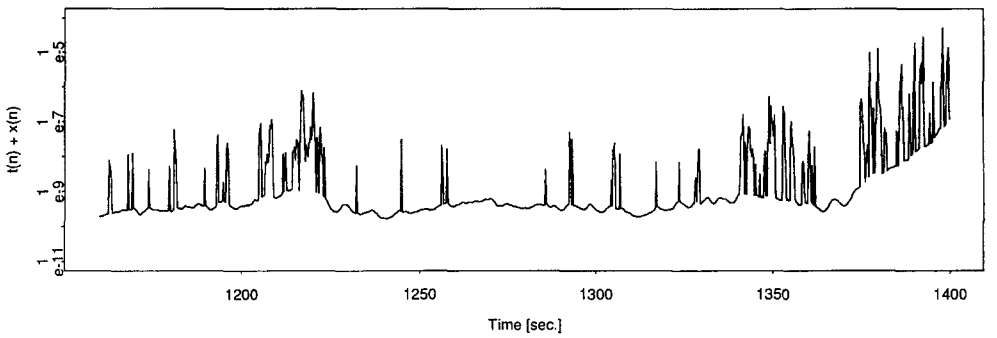

(b)

Fig. 10. (a) Observation $y(n)$ for 100 [Hz] in time domain. (b) The cleaned data, $t^*(n) + x(n)$.

two groups, group-B and of group-$B + x$, which is essentially based on the ratio of the signal to the background noise intensity at each θ.

We present in Fig. 10(b) the cleaned data for data points shown in Fig. 10(a). The relatively larger fluctuation of $t^*(n)$ seen in Fig. 10(b) results in the larger variance of $t^*(n)$ seen in Fig. 9(c), compared with that seen in Fig. 7(c). Although $y(n)$ in Fig. 10(a) appears to prevent us from extracting useful information, Fig. 10(b) suggests that our procedure provides us a chance to examine the data strongly contaminated with the spin noise.

6. Discussion

In the first estimation of the phase response function, $\log f^*_{(1)}$, we separate the procedure into two steps: one is to obtain a rough estimate of $\log f_i$ and the other is to smooth it. This separation is needed to remove the data points with a real signal (i.e., the group-$B + x$) in a process for obtaining the *smooth* phase response curve

of the background noise. Namely, the smoothing of $u(n)$ $(= \log y(n) - \log t^*_{(0)}(n))$ in the phase domain requires a rejection of effects from outliers which appear in this study as the data points of the group-$B + x$. This problem has been treated in the framework of a time (and space) series analysis as the modeling of the "robust filter (smoother)" which is designed to give a good estimate for a trend in the presence of outliers. The running median smoother (Tukey (1977)) is commonly used for the robust (nonlinear) smoother. In the course of our study, we applied this smoother to our data, but we found that it fails to exclude the outliers. The unsuitability of this method for our data stems from the fact that there exist several outliers (corresponding to the data of the group-$B + x$) within a narrow phase range; i.e., the bulk of natural emissions is often observed within a limited phase range. As for another robust filter, the non-Gaussian state-space modeling has received much attention, because it can accommodate the outliers systematically. The outlier in our problem is referred to in the non-Gaussian state-space approach as additive outliers (AO) which are observed in the observation noise (Tsay (1986)). Although we assume that the phase response function shows a smooth behavior without discontinuities, the data set for the lowest electric field channel such as 100 [Hz] sometimes shows a few abrupt jumps in the trend. In this case, we have to consider a more general model of the AO + IO type for the nonlinear smoothing, where IO denotes the innovations outlier. Except for the special case which sometimes occurs in the lowest channel, we have only to deal with the AO model in this study.

The method proposed by Kitagawa (1987), which is an AO + IO type model, has great potential for application to many fields, because of its simplicity which can be realized by the direct modeling of an observation scheme as well as by the numerical computations necessary for the filtering and smoothing algorithms. Furthermore, his model excels in an objective choice of the tradeoff between the smoothness and goodness of fit according to the information criterion, ABIC. The occurrence of the additive outlier which is in fact the observation with a real signal (group-$B + x$) can be characterized in his model by some appropriate noise distribution with a heavy weight on the positive side. Of course, this noise distribution is chosen to maximize ABIC.

In our case, it is not possible to directly apply his method, because, as previously mentioned, our data are irregularly spaced in the phase domain and so we have to conform the data set to the equispaced format in his model. The easiest way is to neglect the fact that the data are not equispaced. Even if we adopt this alleviation, another difficulty due to the large data length ($10^4 < N$) arises in the limited computational memory on the workstation such as a SPARCstation. Of course, we can now solve this problem by using a supercomputer, but we intend to develop the program for use as part of the data reduction process, which is typically carried out with small computers such as workstations. Hence, we do not adopt his method for nonlinear smoothing.

The smooth spline function is extremely useful for fitting the irregularly spaced data. Although in our case the treatment of the AO should be included in a procedure of estimating the coefficients in spline functions, the most commonly used method for a smooth spline function is based on an assumption that data

contain no additive outlier (Wahba and Wold (1975), Wahba (1975, 1990), Ishiguro and Arahata (1982), Silverman (1984, 1985)). Even if we adopt a spline function to represent the phase response while taking care of the presence of the AO, the merits of using the spline function at the expense of huge computing time cannot be justified in our case where the data points are densely and uniformly scattered in phase domain. Moreover, since there are so many data points ($M_i \sim 60$) within a small phase range such as $\Delta\theta = 1$ in which the phase response function is assumed to be almost constant, the irregular space between data points in the phase domain forces us not to use a spline function.

The smoothing in phase domain in the presence of the outlier is attributed to the AO type modeling. The treatment of the outliers which appears in smoothing $e^*_{(k+1/2)}$ $(k = 0, 1, \ldots)$ also requires the AO type model capable of automatically accommodating the outlier in smoothing. As previously mentioned, we smooth $e^*_{(k+1/2)}$ in the time domain to extract the slowly changing (trend) component in $e^*_{(k+1/2)}$. The value of $e^*_{(k+1/2)}$ for the group-$B + x$, which is quite far separated from the bulk composed of the group-B, significantly affects the estimated trend component when we simply apply the linear filter in which the estimate is defined by a weighted linear combination of $e^*_{(k+1/2)}$. Of course, the smoothing based on the Bayesian approach with Gaussian noise is also classified as the linear filter (Silverman (1985), Higuchi (1991*a*)). In addition, an effect of $e^*_{(k+1/2)}$ for the group-$B + x$ on the optimization of tradeoff parameter (so-called hyperparameter) becomes serious. The treatment used in our study is implicitly based on an assumption that the distribution of $e^*_{(k+1/2)}$ within a range of $e_{\min}$–$e_{\max}$ could be satisfactorily approximated by a Gaussian. A choice of $e_{\min}$ is quite reasonable because minimum value of $e^*_{(k+1/2)}$, $e_{\min}$, is definitely classified into group-B from a physical point of view. In contrast, a selection of $e_{\max}$ is somewhat *ad hoc* and cannot be justified only by the assumption of the Gaussian distribution.

To solve these problems, the non-Gaussian method proposed by Kitagawa (1987) is quite adequate, because any distribution for the observation noise is, in his method, realized by a piecewise linear function and so the histogram of $e^*_{(k+1/2)}$ could be adopted for the most appropriate observation noise model. Unfortunately, the large data length also burdens this approach due to the large computational memory required. In order to mitigate this problem, we do not apply the smoother algorithm but instead replace the estimate by that obtained by the filtering algorithm. However, even if we adopt this approach which requires more computational time rather than the normal linear smoothing approach, there is substantially little difference in the smoothed $e^*_{(k+1/2)}$ between our method and the general one proposed by Kitagawa (1987). The reason is that the distribution of $e^*_{(k+1/2)}$ within the range less than $e_{\max}$ can be sufficiently approximated by a Gaussian. Of course, there still remains a problem of the most reasonable choice of $e_{\max}$ assigned to the maximum fluctuation of the background noise in positive direction. We fully agree with Kitagawa (1987) that both the broad applicability and simplicity of his model compensates for the computational costs. Fortunately, this problem of a choice of $e_{\max}$ is not substantial in our case, because there is no point, at most a few points, around $e_{\max}$, for most of cases in our data set. In short, the outliers classified into the group-$B + x$ are sparsely spaced within the

range of much larger than $e_{\max}$. In addition, our objective in this study is not a precise estimate of the background noise intensity, but the automatic and quick extraction of the natural emissions (real signal). We therefore do not adopt his method.

In this study, we assume that the background noise can be described as a function of time, n, and phase, $\theta(n)$, and took the simplest form for its representation: $B(n,\theta) = I(n)f(\theta(n)) = w(n)t(n)f(\theta(n))$. This simplification can be justified from many examinations of data which show that the logarithm of the observations without a natural emission shows a dependency only on phase after removing the long-term trend in the background noise intensity. More specifically, the form of $\log f(\theta)$ can be assumed to be constant as a function of time. This model directly and naturally reflects our knowledge obtained from detailed inspection of many data. However, there occasionally occurs a gradual change in $\log f(\theta)$, which cannot be described by our models. This inability can be resolved by considering more general expressions for the background noise as a function of time and phase. Namely, we divide the total data into sub-intervals and assume that the background noise is constant during each interval ΔP. In addition, we add a prior notion such that $B(n+\Delta P,\theta) \sim B(n,\theta)$ and $B(n,\theta) \sim B(n,\theta+\Delta\theta)$. This approach can be realized by quantizing $B(n,\theta)$ as $B(n,i\Delta\theta)$ or by representing it in terms of a spline function, in the phase domain. In this approach, the major difficulties stem both from the huge computational memory required for its numerical realization and from the computing time necessary for obtaining an optimal $B(n,\theta)$ according to ABIC.

Acknowledgements

The electric field data examined in this report were obtained by the Pioneer Venus orbiter and were processed with support furnished by the National Aeronautics and Space Administration under research grants NAG2-501 and NAG2-485.

References

Akaike, H. (1980). Likelihood and the Bayes procedure (with discussion), *Bayesian Statistics*, 143–165, University Press, Valencia, Spain.

Gersch, W. and Kitagawa, G. (1988). Smoothness priors in time series, *Bayesian Analysis of Time Series and Dynamic Models* (ed. J. C. Spall), 431–476, Marcel Dekker, New York.

Grubbs, F. E. (1969). Procedures for detecting outlying observations in samples, *Technometrics*, **11**, 1–21.

Higuchi, T. (1991*a*). Frequency domain characteristics of linear operator to decompose a time series into the multi-components, *Ann. Inst. Statist. Math.*, **43**, 469–492.

Higuchi, T. (1991*b*). Method to subtract an effect of the geocorona EUV radiation from the low energy particle (LEP) data by the Akebono (EXOS-D) satellite, *Journal of Geomagnetism and Geoelectricity*, **43**, 957–978.

Higuchi, T., Kita, K. and Ogawa, T. (1988). Bayesian statistical inference to remove periodic noise in the optical observations aboard a spacecraft, *Applied Optics*, **27**, 4514–4519.

Ishiguro, M. and Arahata, E. (1982). A Bayesian spline regression, *Proc. Inst. Statist. Math.*, **30**, 29–36 (in Japanese).

Kita, K., Higuchi, T. and Ogawa, T. (1989). Bayesian statistical inference of airglow profiles from rocket observational data: comparison with conventional methods, *Planet Space Sciences*, **37**, 1327–1331.

Kitagawa, G. (1979). On the use of AIC for the detection of outliers, *Technometrics*, **21**, 193–199.

Kitagawa, G. (1987). Non-Gaussian state space modeling of nonstationary time series (with discussion), *J. Amer. Statist. Assoc.*, **79**, 1032–1063.

Kitagawa, G. and Akaike, H. (1982). A quasi Bayesian approach to outlier detection, *Ann. Inst. Statist. Math.*, **34**, 389–398.

Russell, C. T. (1991). Venus lightening, *Venus Aeronomy*, 317–356, Kluwer Academic Publishers, Dordrecht.

Scarf, F. L. and Russell, C. T. (1988). Evidence of lightning and volcanic activity on Venus: Pro and Con, *Science*, **240**, 222–224.

Scarf, F. L., Taylor, W. W. L., Russell, C. T. and Elphic, R. C. (1980). Pioneer Venus plasma wave observations: the solar wind interaction, *Journal of Geophysical Research*, **85**, A13, 7599–7612.

Silverman, B. W. (1984). Spline smoothing: the equivalent variable kernel method, *Ann. Statist.*, **12**, 898–916.

Silverman, B. W. (1985). Some aspects of the spline smoothing approach to non-parametric regression curve fitting (with discussion), *J. Roy. Statist. Soc. Ser. B*, **47**, 1–52.

Strangeway, R. J. (1991). Plasma waves at Venus, *Space Science Review*, **55**, 275–316.

Tietjen, G. L. and Moore, R. H. (1972). Some Grubbs-type statistics for the detection of several outliers, *Technometrics*, **14**, 583–597.

Tsay, R. S. (1986). Time series model specification in the presence of outliers, *J. Amer. Statist. Assoc.*, **81**, 132–141.

Tukey, J. W. (1977). *Exploratory Data Analysis*, Addison-Wesley, Reading, Massachusetts.

Wahba, G. (1975). Smoothing noisy data with spline functions, *Numer. Math.*, **24**, 383–393.

Wahba, G. (1990). *Spline Models for Observational Data*, Society for Industrial and Applied Mathematics, Philadelphia, Pennsylvania.

Wahba, G. and Wold, S. (1975). A completely automatic French curve—Fitting spline functions by cross validation, *Comm. Statist.*, **4**, 1–17.